Variation in Convective and Radiative Heat Transfer with Reynolds Number and Temperature in a Backward-Facing Step Combustor

Jennifer Colborn* and Jacqueline O'Connor†
Pennsylvania State University, University Park, PA, 16802, USA

Flow fields in gas turbine combustors have a wide variety of flow features near the combustor liner, including recirculation, shear layer separation and impingement, and boundary-layer development. As a result, modeling and predicting the heat transfer to the liner is challenging. The current work seeks to investigate the relative contributions of convective and radiative heat transfer to combustor liners using a backward-facing step combustor over a range of flow conditions. Reynolds number and air temperature were varied to determine the variation of recirculation zone length. Understanding the recirculation zone location is important for sensor placement for the next step of experiments. Length of the recirculation zone does not change with varying Reynolds number or temperature when considering the natural variation due to the unsteady shear layer formed off the step. After determining the recirculation zone length, the experiment will be instrumented with a heat flux sensor and radiometer to determine the relative impact of radiation and convection through the combustor.

I. Nomenclature

h	=	step height, 2 cm
PIV	=	Particle Image Velocimetry
Re_h	=	step height Reynolds Number
T_{air}	=	air temperature
v_x	=	streamwise velocity
x, y, z	=	streamwise, wall-normal, and spanwise directions coordinate, respectively
X_r	=	recirculation zone length
μ	=	dynamic viscosity
ρ	=	density

II. Introduction

.

Flow fields in gas turbine combustors have a wide variety of flow features near the combustor liner, including recirculation, shear layer separation and impingement, and boundary-layer development, making modeling and predicting the heat transfer to the liner challenging. Most studies considering combustor liner heat transfer are non-reacting and only capture convective heat transfer; the goal of many of these studies is to assess liner cooling strategies [1–4]. While these studies highlight the importance of combustor flow field dynamics, the impact of radiative heat transfer is neglected, which has been shown to be important with a flame present [5–7]. To address this discrepancy, the current work seeks to investigate the relative contributions of convective and radiative heat transfer to combustor liners using a backward-facing step combustor over a range of flow conditions.

Backward-facing step combustors have been previously used in combustion studies as they contain many of these relevant combustor flow field features in a relatively simple two-dimensional geometry [8, 9]. A shear layer separates from the trailing edge of the step and impinges on the bottom wall, creating a recirculation region as well as a new boundary layer on the bottom wall as the flow "recovers." A flame can stabilize within the shear layer and drive convective

*Graduate Research Assistant, Mechanical Engineering, AIAA Student Member.
†Associate Professor, Mechanical Engineering, AIAA Associate Fellow.

and radiative wall heat transfer. Previous studies of convective heat transfer in this geometry have shown reduced heat transfer within the recirculation zone, increased heat transfer in the recovery region [3], and up to two times the heat transfer at the shear-layer impingement location [10], as shown in Figure 1. These features are similar to those seen in a combustor, but with a simplified geometry that allows for increased diagnostics and simplified modeling. Previous heat transfer research with backward-facing steps has shown increased heat transfer downstream of the recirclation zone, and Ge et al. [11] demonstrated increased heat transfer at the shear layer with a flame as opposed to hot gases, most likely due to flame stabilization in the shear layer. However, these studies neglect the effects of radiation within the flow.

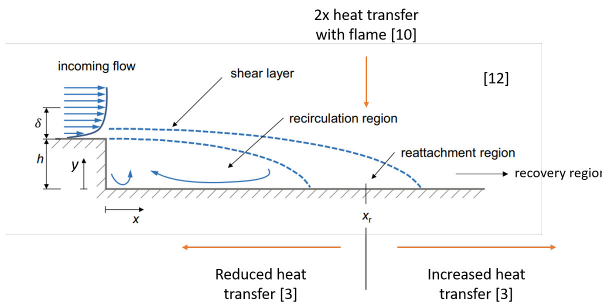

Fig. 1 Convective heat transfer variation across a backward-facing step flow [12]

To fill in the experimental gap, a backward-facing step combustor will be used to determine the relative impact of radiative and convective heat transfer. Using tightly-coupled experiments and models, the relative impact of these heat transfer modes will be determined along with the necessary model fidelity to capture the behavior. In this study, we use simultaneous measurements of total heat flux and radiative heat flux (using a radiometer) over a range of flow Reynolds numbers and gas temperatures to measure the heat transfer to the wall in a range of locations. Companion large-eddy simulation is used to better understand the changes in heat transfer over this parameter space.

III. Experimental Design

The backward-facing step experiment used was designed consistently with historical experiments; a detailed discussion of the rig is provided in Toumey et al. [13], and so a shorter overview is provided here. The experiment features a preconditioning section, as shown in Figure 2, to allow for preheating the flame and particle injection, as well as a combustor that is optically accessible on three sides with fused silica windows.

The overall combustor dimensions are 5.8 cm high by 30 cm long by 19 cm wide, as shown in Figure 3. Characterization of this combustor using particle image velocimitry has shown two-dimensional flow through the center of the combustor, allowing for diagnostics on both sides of the centerline as well as a smaller computational domain [13].

Air was injected into the experiment in two locations: into the preconditioning section at the vitiator and through additional injection points located approximately 20 cm upstream of the combustor. For observation of hot flow characteristics, the flow was vitiated upstream using methane. Fuel was injected in two locations: premixed into the main air supply and directly injected around the igniter. A high-voltage igniter was used for ignition. To ignite the experiment, the main air was preset to 300 SLM with no fuel being premixed. Pilot fuel set to 20 SLM and the igniter were turned on simultaneously to light the pilot flame. The vitiator was found to ignite consistently at this condition, so all tests started at this condition. The flame was then stabilized by decreasing the pilot injection to 10 SLM and adding 24 SLM premixed into the main airflow, and the vitiator was ran for three minutes to allow the experiment to warm up, after which the desired test condition was reached.

Velocity field data is collected using a high-speed particle image velocimity (PIV) system with techniques the same as those used previously [13]. A Nd:YAG laser operating at 532 nm cast a laser sheet using mirrors and a LaVision sheet forming optic, with a camera (Photron FASTCAM SA1.1) 90 degrees to the laser sheet. Equipped with a 60 mm f/2.8 AF Micro Nikon lens and a laser line filter (Edmund Optics TECHSPEC 532nm CWL), the camera collected images at 5 kHz in double-frame mode with a pulse separation of 80 μs. Aluminum oxide particles are used for seeding the flow field with diameters of 0.5-2.0 μm. Vector calculations were performed from Mie scattering images using LaVision's DaVis 8.3 with a multi-pass algorithm with varying window sizes ranging from 64x64 to 16x16 and 50% window overlap. 5000 vector fields are collected at each condition.

Due to the size of the combustor, a single laser sheet could not be used to capture the entire frame. Four different

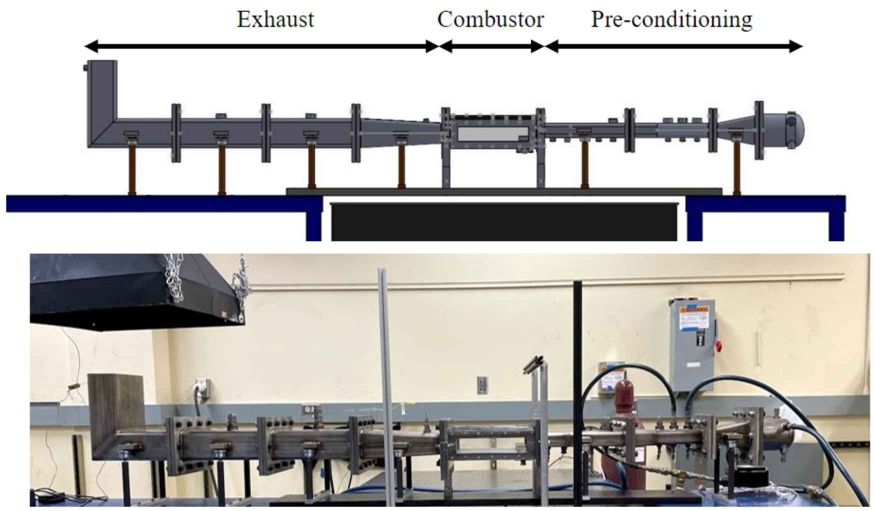

Fig. 2 A schematic of the experimental configuration.

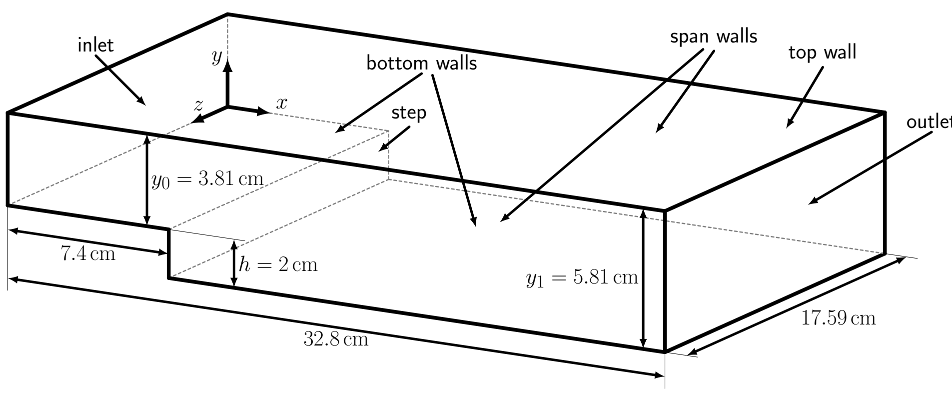

Fig. 3 Combustor dimensions

sampling images were collected to capture the velocity performance of the entire combustor. PIV data was collected on consecutive days using the same test procedures to ensure similar combustor behavior. Once the combustor had reached the desired condition, PIV collection was triggered, collecting 5000 image pairs. A sample resulting velocity field is shown in Figure 4, where pink lines denote the boundaries between the different collection regions, and the white line represents the zero-velocity contour of the recirculation zone.

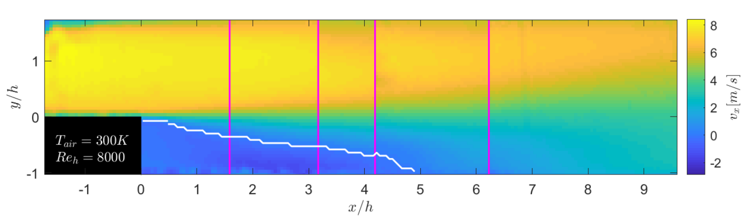

Fig. 4 Sample velocity field, taken at $Re_h = 8000$ and $T_{air} = 296K$

IV. Initial Results

Before characterization of heat transfer between the recirculation, impingement, and recovery zones can be completed, the behavior of the recirculation zone within the combustor needs to be understood for proper instrumentation. Initial sampling conditions show a wide range of achievable temperatures, as shown in Figure 5. The flow was seeded with the dilution air in the current experimental configuration, which accounted for 6-16% of the total flow, limiting the range of temperatures used for testing. Further experiments with particle image velocimetry diagnostics were performed over a range of both Reynolds numbers and temperatures shown in Table 1 to determine the change in recirculation zone length with both Reynolds Number (Re_h) and temperature. Reynolds number, which was calculated with respect to the step height h, was varied by 1000 from 3000 to 8000, and temperatures were also varied using the test procedures detailed as a result of the selected air and fuel flow rates for observation.

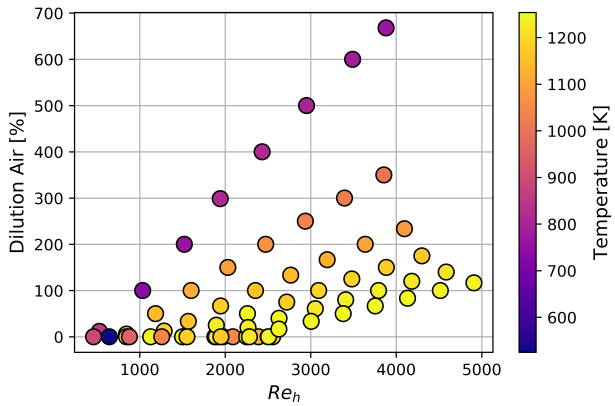

Fig. 5 Temperature operability, sampled 2.5cm upstream of the combustor entrance

Table 1 Experiment Test Conditions

Case	$Re_h = \frac{\rho v_x h}{\mu}$	$T_{air}\,[K]$
1	3000-8000	296
2	2056	926
3	2277	1132
4	2553	1220

Results of the PIV measurements showed that in this experiment the recirculation zone length, X_r, does not widely vary with changing Reynolds number. The time-averaged recirculation zone length was calculated by time-averaging the velocity fields and calculating the time-averaged zero-velocity contour along the edge of the recirculation zone. Where that zero-velocity contour intersects the bottom wall of the experiment is the recirculation zone length. Observation of the velocity results indicated that the recirculation zone length varies in time, however, and so a variance of recirculation zone length is also calculated. The recirculation zone variance was calculated by averaging every ten velocity fields, applying a median filter to the velocity data, and searching for the zero-velocity location at the bottom wall of the combustor. The results of these calculations are shown in Figure 6, where the time-averaged recirculation zone length is relatively constant across all observed Reynolds numbers, as is the variation in recirculation zone length. Capturing this variation is important for interpretation of the heat transfer results at different locations, as the convective heat transfer in a recirculation zone can be quite different than that downstream of recirculation.

Variation of the inlet temperature, as indicated in Table 1, also does not have a significant effect on the recirculation zone length. Figure 7 shows the variation in time-averaged recirculation zone length and standard deviation as a function of inlet temperature. The length decreases slightly between the cold-flow and hot-flow conditions, but then does not vary much at the higher temperatures. Similar to the Reynolds number study discussed previously, the standard deviation in recirculation zone length does not vary significantly with temperature.

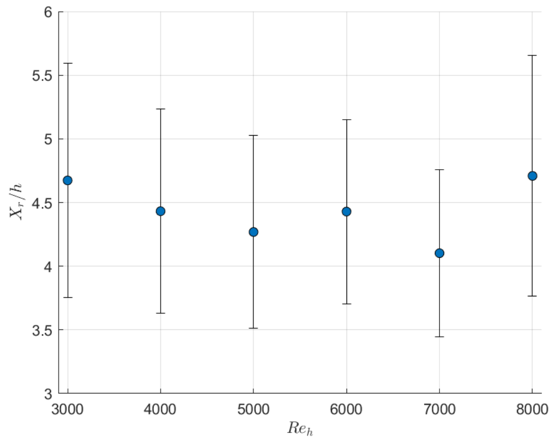

Fig. 6 Time-averaged recirculation length variation with Reynolds number at T_{air} = $296K$. One standard deviation is reported by vertical bars.

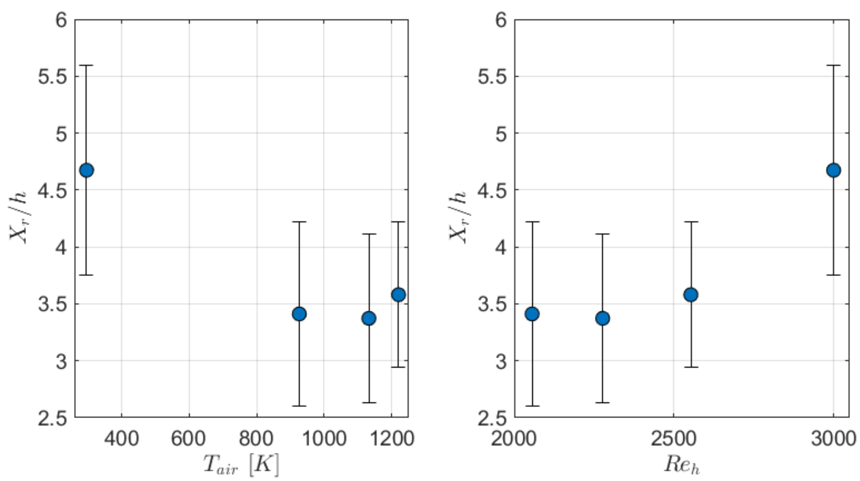

Fig. 7 (a) Recirculation length change with temperature, and (b) recirculation length variation with Reynolds number.

V. Next Steps

From the recirculation length information gathered, locations for instrumentation have been determined for further testing. The combustor is being fitted with ports along the length of the combustor for a heat flux gauge and a radiometer (Vatell), as well as several thermocouples. These sensors are Gardon gauges, which consist of a circular-foil transducer to measure heat flux [14]. The radiometer additionally has a sapphire window to filter out only radiation. The sensors can be moved to four different locations along the length of the combustor, allowing for measurement of heat flux in the different flow regions of the combustor. Experiments will be repeated with these gauges to determine the changes to the two different modes of heat transfer over a range of operating conditions.

References

[1] Scrittore, J. J., Thole, K. A., and Burd, S. W., "Investigation of Velocity Profiles for Effusion Cooling of a Combustor Liner," *Journal of Turbomachinery*, Vol. 129, No. 3, 2006, pp. 518–526. https://doi.org/10.1115/1.2720492, URL https://doi.org/10.1115/1.2720492.

[2] Andreini, A., Becchi, R., Facchini, B., Mazzei, L., Picchi, A., and Turrini, F., "Adiabatic effectiveness and flow field

measurements in a realistic effusion cooled lean burn combustor," *Journal of Engineering for Gas Turbines and Power*, Vol. 138, No. 3, 2016. https://doi.org/10.1115/1.4031309.

[3] Tarchi, L., Facchini, B., Maiuolo, F., and Coutandin, D., "Experimental investigation on the effects of a large recirculating area on the performance of an effusion cooled combustor liner," *Journal of engineering for gas turbines and power*, Vol. 134, No. 4, 2012. https://doi.org/10.1115/1.4004729.

[4] Berger, S., Richard, S., Staffelbach, G., Duchaine, F., and Gicquel, L., "Aerothermal prediction of an aeronautical combustion chamber based on the coupling of large eddy simulation, solid conduction and radiation solvers," *ASME Turbo Expo 2015: Turbine Technical Conference and Exposition*, American Society of Mechanical Engineers Digital Collection, 2015. https://doi.org/10.1115/GT2015-42457.

[5] Andreini, A., Caciolli, G., Facchini, B., Picchi, A., and Turrini, F., "Experimental Investigation of the Flow Field and the Heat Transfer on a Scaled Cooled Combustor Liner with Realistic Swirling Flow Generated by a Lean-Burn Injection System," *J. Turbomach.*, Vol. 137, No. 3, 2015. https://doi.org/10.1115/1.4028330.

[6] Bailey, J., Intile, J., Fric, T., Tolpadi, A., Nirmalan, N., and Bunker, R., "Experimental and Numerical Study of Heat Transfer in a Gas Turbine Combustor Liner," *J. Eng. Gas Turbines Power*, Vol. 125, No. 4, 2003, pp. 994–1002. https://doi.org/10.1115/1.1615256.

[7] Patil, S., Sedalor, T., Tafti, D., Ekkad, S., Kim, Y., Dutta, O., Moon, H.-K., and Srinivasan, R., "Study of Flow and Convective Heat Transfer in a Simulated Scaled up Low Emission Annular Combustor," *J. Therm. Sci. Eng. Appl.*, Vol. 3, No. 3, 2011. https://doi.org/10.1115/1.4004531.

[8] Altay, H. M., Speth, R. L., Hudgins, D. E., and Ghoniem, A. F., "Flame–vortex interaction driven combustion dynamics in a backward-facing step combustor," *Combustion and Flame*, Vol. 156, No. 5, 2009, pp. 1111–1125. https://doi.org/10.1016/j.combustflame.2009.02.003.

[9] McManus, K., Vandsburger, U., and Bowman, C., "Combustor performance enhancement through direct shear layer excitation," *Combustion and Flame*, Vol. 82, No. 1, 1990, pp. 75–92. https://doi.org/10.1016/0010-2180(90)90079-7.

[10] Vogel, J., and Eaton, J., "Combined Heat Transfer and Fluid Dynamic Measurements Downstream of a Backward-Facing Step," *J. Heat Transfer*, Vol. 107, No. 4, 1987, pp. 922–929. https://doi.org/10.1115/1.3247522.

[11] Ge, B., Ji, Y., Chi, Z., and Zang, S., "Effusion cooling characteristics of a model combustor liner at non-reacting/reacting flow conditions," *J. Appl. Thermal Eng.*, Vol. 113, 2017, pp. 902–911. https://doi.org/10.1016/j.applthermaleng.2016.11.049.

[12] Scharnowski, S., Bolgar, I., and Kahler, C., "Characterization of Turbulent Structures in a Transonic Backward-Facing STep Flow," *Flow Turbulence Combust.*, Vol. 98, 2017, pp. 947–967. https://doi.org/10.1007/s10494-016-9792-8.

[13] Toumey, J., Zhang, P., Zhao, X., Colborn, J., and O'Connor, J. A., "Assessing the wall effects of backwards-facing step flow in tightly -coupled experiments and simulations," *AIAA SciTech 2022 Forum*, American Institute of Aeronautics and Astronautics, 2022. https://doi.org/10.2514/6.2022-0822.

[14] Gardon, R., "An Instrument for the Direct Measurement of Intense Thermal Radiation," *Rev. Sci. Instrum.*, Vol. 24, No. 5, 1953, pp. 366–370. https://doi.org/10.1063/1.1770712.